THE ASTROPHYSICAL JOURNAL, 320:573–585, 1987 September 15

FAR-INFRARED MEASUREMENTS OF N/O IN H II REGIONS: EVIDENCE FOR ENHANCED CN PROCESS NUCLEOSYNTHESIS IN THE INNER GALAXY

D. F. LESTER AND H. L. DINERSTEIN
Department of Astronomy, University of Texas at Austin
M. W. WERNER
Space Sciences Division, NASA Ames Research Center
D. M. WATSON
Department of Physics, California Institute of Technology
R. GENZEL
Department of Physics, University of California at Berkeley
AND
J. W. V. STOREY
Department of Physics, University of New South Wales
Received 1986 October 6; accepted 1987 February 3

ABSTRACT

Measurements of the [N III] 57.3 μm, [O III] 51.8 μm, and 88.4 μm fine-structure emission lines, obtained with the Kuiper Airborne Observatory, are presented for 13 Galactic H II regions spanning a large range in galactocentric distance, and also for two H II regions in the 30 Doradus complex of the LMC. These measurements are combined with data from earlier studies and, using newly revised atomic constants, N^{++}/O^{++} ionic ratios are derived for each of these nebulae. We argue that this ratio is proportional to the elemental ratio N/O, and its differences around the Galaxy reflect differences in nucleosynthetic history. This abundance indicator is compared with O/H and $^{12}C/^{13}C$ in an effort to assemble a consistent picture of nuclear enrichment of nitrogen and oxygen in the disk of our Galaxy.

Using the newest set of atomic constants, the ratio of the 57.3 μm line of [N III] to the 51.8 μm line of [O III] is shown to equal the true ionic ratio N^{++}/O^{++} to within $\pm 25\%$ for any likely electron temperature or electron density. This is a result of the near coincidence of their critical densities to collisional deexcitation. These lines are conveniently juxtaposed in the spectrum, and their diagnostic value to studies of ionization structure and nebular abundances is thus considerable. If the 88.4 μm line of [O III] is measured as well, the effects of collisional deexcitation can be corrected entirely, and the ionic ratio can be derived with great accuracy.

We find that N/O varies significantly with galactocentric distance. The observed H II regions inside 7 kpc have N/O that is, on the average, a factor of 3 higher than those we observe at larger radii. The H II region G337.1 − 0.4 has N/O that is a factor of more than 4 higher than H II regions in the solar circle. The nuclear H II region Sgr A has N/O similar to that for regions in the "5 kpc ring" of enhanced star formation. The region G0.5 − 0.0, at a galactocentric distance of only 100 pc, has N/O about a factor of 2 higher than Sgr A, and is one of the highest of the entire sample. It is not clear which, if either, of these two sources has abundances that are typical of the greater Galactic center region. Our upper limit to the N/O ratio for the LMC is approximately a factor of 10 lower than for the disk of our Galaxy, which is consistent with optical measurements.

Comparison of the inferred N/O with O/H gives evidence for secondary enrichment of nitrogen in the heavily processed regions of the inner Galaxy. This scenario is that expected for nitrogen production by quiescent CN processing in stellar envelopes. Our N/O values also correlate well with molecular measurements of $^{13}C/^{12}C$, a fact which strongly supports a CN-processing mechanism. While recent optical studies have suggested a primary origin for nitrogen in metal-poor systems, our results indicate that secondary production dominates for higher metallicities. The evidence for elevated abundances in the galactic center and 5 kpc ring, where star formation is currently active, suggests that this enhanced star-formation activity has persisted for at least 10^7–10^8 yr.

Subject headings: galaxies: abundances — infrared: spectra — nebulae: abundances — nebulae: H II regions — nucleosynthesis

I. INTRODUCTION

In a previous paper (Lester *et al.* 1983, hereafter Paper I), it was shown that measurements of the far-infrared fine-structure lines [O III] 88.4 μm, 51.8 μm, and [N III] 57.3 μm are useful for measuring the abundances of nitrogen and oxygen in the Galaxy. These lines sample the primary ionic states of these elements in galactic H II regions, are insensitive to electron temperature, and offer the distinct advantage over optical and UV studies of not being affected by interstellar extinction. This last property makes it possible to assay H II regions over much of the disk of our Galaxy.

These lines are, however, collisionally deexcited at moderate

densities ($n_e \approx 10^2$–10^3 cm^{-3}) and as a result, their emissivities are weighted differently than that of hydrogen free-free or recombination emission along any column through a typical nebula which can be assumed to be optically thin to these lines. This effect makes it difficult to determine O^{++}/H^+ and N^{++}/H^+ values with an an accuracy that suits the needs of galactic nucleosynthesis models. The dependence of their emissivities on electron density is similar enough, however, that these far-infrared lines give N^{++}/O^{++} with confidence. As we will show below in § III, current estimates of the atomic constants for these lines allow this ratio to be determined with remarkably high accuracy. To the extent that the ionization equilibrium in the nebula is understood, this ratio should be indicative of the elemental ratio N/O in H II regions.

The N/O abundance ratio has special significance for galactic nucleosynthesis models. Simple models of chemical evolution have suggested that the dominant isotope of nitrogen (^{14}N) is produced primarily by CN processing in stars that have already been seeded with carbon from previous stellar generations. The dominant isotope of oxygen (^{16}O), on the other hand, is expected to be produced in quiescent carbon-burning layers in massive stars. The oxygen yield from these layers is not strongly tied to the amount of light metals with which the star was originally formed. In this picture, in which nitrogen is thus termed a "secondary" element and oxygen a "primary" element, the ratio N/O is a measure of the extent of nuclear processing that a given parcel of gas has undergone (see, for example, Audouze and Tinsley 1976). Observational studies over the last 10 years, however, indicate that this model is not adequate. With the simplifying assumption of instantaneous recycling of enriched ejecta into new stars, the model predicts N/O $\propto$ O/H, which is indicated only marginally from optical studies of spiral-arm H II regions in the optically accessible outer disk of our Galaxy as well as in several external galaxies (see review by Peimbert 1979; also Pagel and Edmunds 1981; Shaver *et al.* 1983; Dufour 1984). These studies, as well as work on metal-deficient stars (Tomkin and Lambert 1984), indicate that, whether or not secondary production of nitrogen is presently dominant in the solar neighborhood, a substantial fraction of this element must have originated by primary processes, perhaps in an initial high-mass generation of stars in the young disk.

From optical studies of relatively nearby H II regions and planetary nebulae, the existence of a negative radial gradient of O/H in the Galaxy now seems well established (see references cited above). This indicates that the cumulative amount of past star formation at a given galactocentric radius decreases with increasing galactocentric radius (R_G), an indication that is supported by measurements of heavy metal abundances in disk stars (Mayor 1976) as well. This radial gradient d log (O/H)/d log (R_G) is only about -0.07 kpc^{-1}, however, and since optical measurements cannot probe abundances at galactocentric distances smaller than about 7 kpc, the total range in directly observed galactic disk abundances is small. A number of indirect abundance indicators, including radio recombination-line electron temperatures of H II regions (Shaver *et al.* 1983; Garay and Rodriguez 1983; Wink, Wilson, and Bieging 1983) suggest, however, that enhanced abundances of primary coolants like oxygen are even more pronounced in the inner Galaxy. In Paper I we showed that one H II complex in this region, W43 at $R_G = 5.5$ kpc, had an N/O ratio a factor of at least 2 higher than that in the solar circle, taken here to be $R_G = 10$ kpc. In this paper we present the results of more detailed measurements of the variation of N^{++}/O^{++} with galactic radius, from the Galactic center through the solar circle and out to 12 kpc. In addition, we report observations of H II regions in the Large Magellanic Cloud, which is known from optical studies to have a quite different nucleosynthetic history than the disk of our Galaxy. Brief preliminary discussions of our results have been given by Dinerstein *et al.* (1984), Dinerstein (1986), and Watson (1986). Our analysis benefits from new data on atomic parameters that has become available since our first paper. Our new results show that the N/O enhancement originally inferred for W43 is indeed representative of abundances in the inner Galaxy. These measurements are compared with independent indicators of elemental and isotopic abundances in an effort to assemble a consistent picture of nuclear enrichment in the inner part of our Galaxy, where star formation is progressing at an especially rapid rate.

II. OBSERVATIONS

The line measurements were made with the UC Berkeley far-infrared Fabry-Perot spectrometer at the Nasmyth focus of the 0.91 m NASA Kuiper Airborne Observatory (KAO). The instrument is described in detail by Storey, Watson, and Townes (1979). The relevant lines and their precise wavelengths are listed in Table 1. The listed wavelength of the [N III] line was redetermined on G333.6−0.2 relative to lines from a sample cell containing $H_2{}^{18}O$ and is probably accurate to about 0.002 μm. The observations presented in this paper were made on flights in 1982 and 1983. The work on the Galactic Center region, southern Galactic H II regions and LMC H II regions were done during the 1983 KAO Australia expedition. The measurements were made in a 50″ diameter FWHM circular beam (effective solid angle 6×10^{-8} sr) with a chop throw of about 4′ in azimuth. Table 2 lists the sources discussed in this paper, in order of galactocentric distance, and the beam positions for the individual objects. The pointing accuracy is estimated to be about $\pm 10''$. For notational consistency, we refer to the H II regions by their G number. Table 2 also cross references these numbers to the more commonly used names of the complexes to which they belong. The galactocentric distances have been taken from the literature and are Schmidt model distances with $R_\odot = 10$ kpc assumed for convenience.

A spectral resolution of one part in several thousand was used for the measurements. This is not sufficient to resolve the (largely thermal) linewidths in these sources, with the exception of Sgr A, and is low enough that thermal continuum radiation

TABLE 1

FAR-INFRARED LINE PARAMETERS

Transition	Wavelength (μm)	A (s^{-1})	$\gamma(10^4$ K)	References
		O^{++}		
$2p^2\ {}^3P_1$–$^3P_0$	88.356	2.62×10^{-5}	0.5417	1, 2
$2p^2\ {}^3P_1$–$^3P_0$	51.815	9.76×10^{-5}	1.2884	1, 2
		N^{++}		
$2p^2\ {}^2P_{3/2}$–$^2P_{1/2}$	57.317	4.77×10^{-5}	1.081	3, 4

REFERENCES.—(1) Aggarwal 1983 (collision strengths); (2) Nussbaumer and Storey 1981 (transition probabilities); (3) Butler and Storey 1987 (collision strengths); (4) Nussbaumer and Storey 1979 (transition probabilities).

TABLE 2

SOURCES OBSERVED

Source	Complex	R.A. (1950)	Decl. (1950)	R_G[a]
G0.0+0.0	Sgr A	$17^h42^m28^s.8$	−28°59′20″	0.0
G0.5−0.0	Sgr B2	17 43 51.0	−28 31 30	0.1
G10.2−0.4	W 31	18 06 26.6	−20 19 50	4.0
G337.1−0.2	...	16 33 01.0	−47 25 18	5.3
G30.8−0.0	W 43	18 45 00.0	−02 00 00	5.5
G25.4−0.2SE	...	18 35 32.8	−06 50 35	6.0
G333.6−0.2	...	16 18 24.5	−49 59 10	7.0
G49.5−0.4	W 51	19 21 23.0	+14 24 55	7.7
G15.0−0.7	M 17	18 17 34.5	−16 13 25	8.6
G209.0−19.3	Orion A	05 32 48.0	−05 25 30	10.5
G75.8+0.4	ON 2	20 19 47.3	+37 21 30	10.8
G111.5+0.8	NGC 7538	23 11 22.9	+61 13 50	11.5
G133.7+1.2	W 3	02 22 57.5	+61 52 55	11.8
MC 77	LMC	05 40 24.0	−69 46 00	...
30 Dor Pk1	LMC	05 39 08.0	−69 06 20	...
30 Dor Pk2	LMC	05 38 53.0	−69 07 50	...
R136a	LMC	05 39 04.0	−69 07 40	...

[a] Galactocentric distances assuming $R = 10.0$ kpc.

is detected for the brighter sources. For all the sources, at least four resolution elements were scanned, and the data were binned in wavelength increments that oversample the resolution element by at least a factor of 10. Particularly interesting examples of our far-infrared line spectra are shown in Figure 1 for G337.1−0.2 and Figure 2 for 30 Doradus. The lines in these objects are among the weakest in our sample, and these figures thus serve to indicate the quality of our data. These spectra, as discussed below, exemplify regions of very different electron density and N^{++}/O^{++}.

Flux calibration was accomplished using continuum measurements. The primary flux calibration is based on the measurements of Saturn by Haas *et al.* (1982), using their model for disk and ring brightness temperatures, and computed for the date of our observations. Secondary calibrations are from the observations of G333.6−0.2 by Hyland *et al.* (1980) and measurements of G0.5−0.0 by Gatley *et al.* (1977). The instrumental responsivity derived from observations of the latter source, which has its calibration pedigree in *Pioneer* spacecraft measurements of Jupiter, agrees very well with that from Saturn. The observations of G333.6−0.2 give consistent responsivities only when those data, calibrated originally against the Loewenstein *et al.* (1977) brightness temperature of Saturn, was rescaled in accordance with the Haas *et al.* value. Where it was well observed, the continuum flux density of an individual program object was given high weight in the calculation of responsivity for that line measurement. The excess continuum signal due to leakage of the low-order Fabry-Perot blocking filter in adjacent orders of the scanning Fabry-Perot was taken into account in the line flux calibration. The effect was smaller than 20% in all cases. The derivation of N^{++}/O^{++} and electron density is not sensitive to the absolute flux density calibration, since the line *ratios* are used for both the density determination and the ionic ratio. In fact, the 57 μm line of [N III] is so close in wavelength to the 52 μm line of [O III] that their flux ratio is almost identical to their equivalent width ratio, so the line flux ratio can be determined independently of flux calibration, if necessary, for a source with measurable continuum. Atmospheric water vapor does not have strong lines that are coincident with any of these three ionic lines, and no correction for water vapor absorption was considered necessary.

The new line fluxes are listed in Table 3, along with previously published values for other regions, germane to this study, made with the same instrument. Fluxes from Paper I have been revised to give them a flux calibration pedigree that is consistent with the new data. Except for especially faint sources, as noted in the table, the errors in the line fluxes are determined by the uncertainty in the responsivity calibration of the instrument, since the signal-to-noise (S/N) ratio of the individual line detections was generally high. This calibration error can be estimated from observations of different continuum sources and is about ±30%. At least half of this error is probably due to calibration errors in the continuum maps from which the standard flux densities were taken. However, the line intensity *ratios* should, in all cases, be accurate to about ±15%. For Sgr A the high-velocity dispersion reduced the line-to-continuum ratio and resulted in some additional uncertainty.

III. ELECTRON DENSITY AND IONIC ABUNDANCE RATIO

The procedure for deriving the ionic ratio N^{++}/O^{++} from measurements of the two far-infrared oxygen lines and the

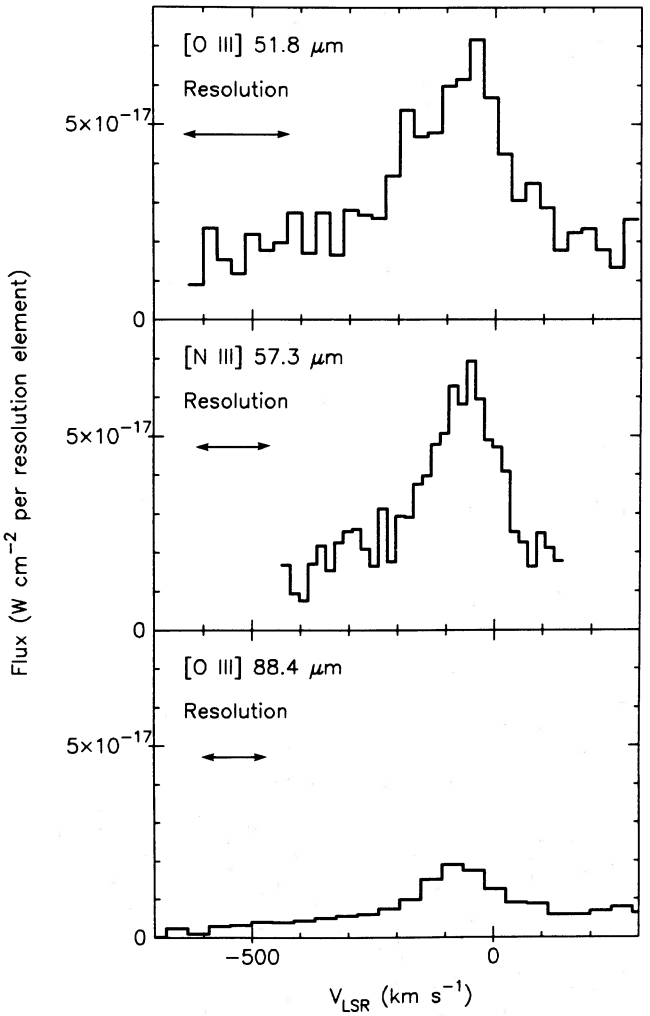

FIG. 1.—[O III] and [N III] fine-structure line detections for G337.1−0.2. This region has a moderately high density compared with most regions that were observed and has the highest N^{++}/O^{++} in our sample.

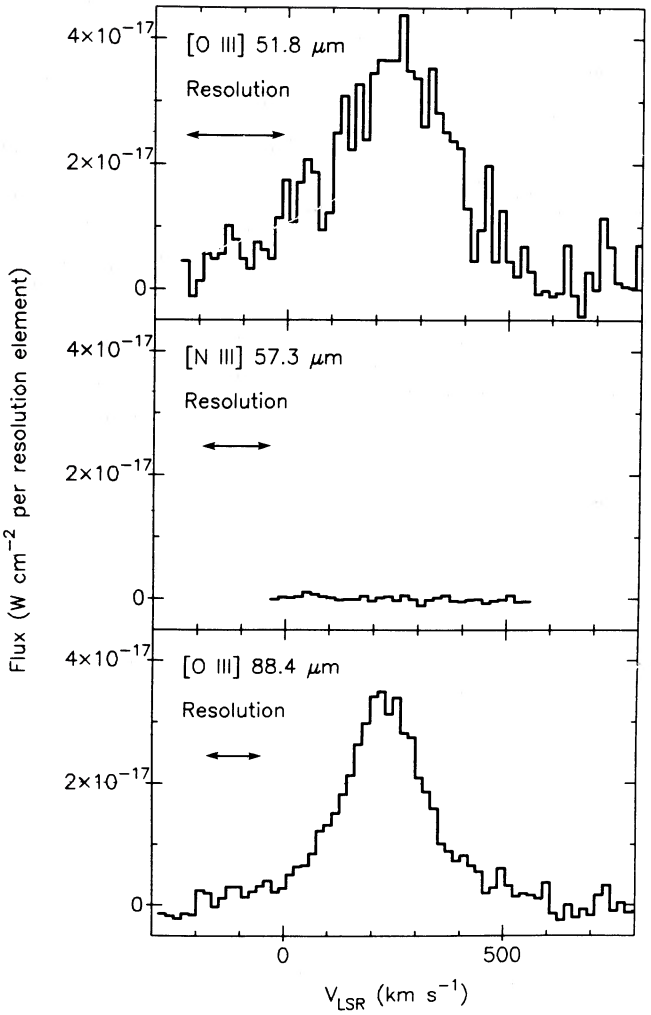

FIG. 2.—[O III] and [N III] fine-structure line detections for 30 Dor Peak 1. This region has a low electron density compared with most regions that were observed and has the lowest N^{++}/O^{++} in our sample.

far-infrared nitrogen line is described in detail in Paper I. Briefly, the ionic ratio is equal to the line flux ratio divided by the emissivity ratio. The latter ratio depends very little on the electron temperature of the gas since $h\nu \ll kT$ for each of the transitions. Due to differences in the critical densities for collisional deexcitation for the three lines there is, however, a residual dependence of the emissivity ratio on the electron density. These dependences are shown graphically for volume emissivity ratios of 57.3 μm/51.8 μm and 57.3 μm/88.4 μm, respectively, in Figures 3 and 4. The two oxygen lines have substantially different electron density dependences, and thus their ratio can be used to generate a measure of the beam-averaged electron density. This electron density value is independent of abundance, and by virtue of their similar ionization potentials is representative of both the O^{++} and N^{++} regions. Thus it can be used to remove the residual electron density dependence in the [N III]/[O III] line ratios. Figure 5 shows the dependence of 51.8 μm/88.4 μm on electron density and electron temperature. The absolute emissivity per unit volume per unit density of the 51.8 μm line is shown in Figure 2 of Dinerstein, Lester, and Werner (1985), in which the behavior of the [O III] lines is discussed in more detail.

TABLE 3

MEASURED LINE FLUXES

Source	52 μm [O III]	57 μm [N III]	88 μm [O III]
	Line flux in units 10^{-17} W cm^{-2}		
G0.0+0.0	5.2 G	2.3	0.7 G
G0.5−0.0	1.4	2.4	1.7
G10.2−0.4	3.1	1.2	2.5
G15.0−0.7	91. W	19. W	39. W
G25.4−0.2SE	14.2	10.4	7.6
G30.8−0.0	14.3 L	6.6 L	7.9 L
G49.5−0.4	79. W	12. W	11. W
G75.84−0.2	...	3.3 L	1.6 L
G111.5+0.8	19. W	7.8	13. W
G133.7+1.2	22.	3.6	5. S
G209.0−19.3	19.3 L	4.3 L	4.9 L
G333.6−0.2	26.7	11.9	5.0
G333.6−0.2 40″N	12.1	3.4	2.9
G337.1−0.2	5.6	6.0	1.9
30 Dor Pk1	7.7	0.2:	7.4
30 Dor Pk2	5.8	0.6:	5.9
R136a	3.1	...	4.3
MC 77	...	...	1.3

Reference to line fluxes (all others from this paper): L: Paper I; S: Storey *et al.* 1979; W: Watson *et al.* 1981; G: Genzel *et al.* 1984.

Figures 3, 4, and 5 are similar to those presented in Paper I except that updated atomic parameters have been used to determine the line emissivities as a function of temperature and density. The variation of collision strengths with temperature has been included in this calculation. Spontaneous transition probabilities for O^{++} are taken from Nussbaumer and Storey (1981) and for N^{++} from Nussbaumer and Storey (1979). The *ab initio* calculation of the *A* values for O^{++} by Baluja and Doyle (1981) gives results that are consistent with those of Nussbaumer and Storey when corrected for the difference between the calculated energy levels and those observed (cf. Nussbaumer and Rusca 1979). Collisional excitation rates (averaged over a Maxwellian electron energy distribution at the appropriate temperature) were taken from Aggarwal (1983)

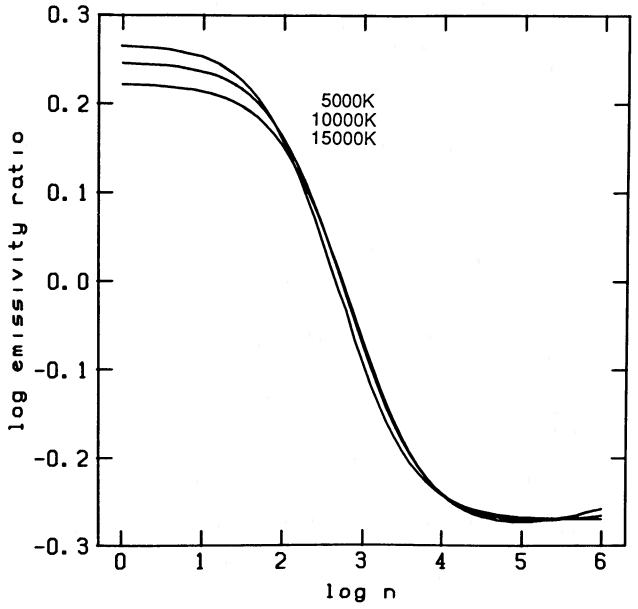

FIG. 3.—Volume emissivity ratio of [N III] 57.3 μm/[O III] 51.8 μm as a function of electron temperature and electron density.

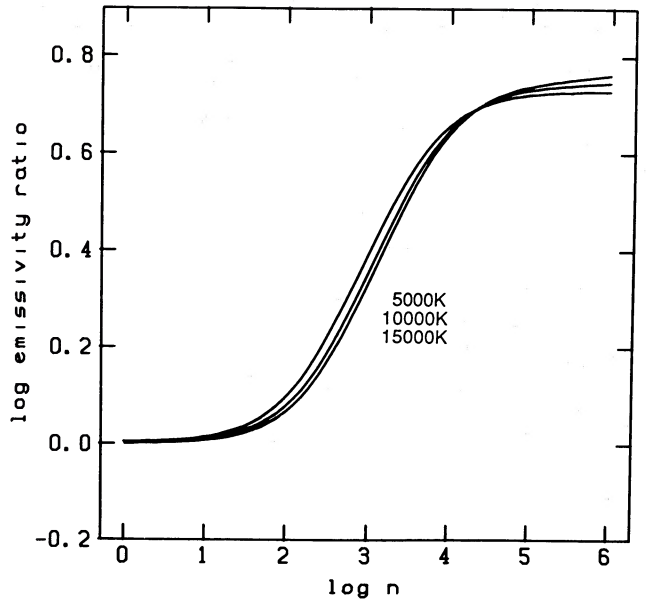

FIG. 4.—Volume emissivity ratio of [N III] 57.3 μm/[O III] 88.4 μm as a function of electron temperature and electron density.

for the O^{++} fine-structure lines, and from Butler and Storey (1987) for N^{++}.

The new N^{++} collision strength from Butler and Storey (1987) is within a few percent of the result of Saraph, Seaton, and Shemming (1969), which was used in Paper I, and it is about 50% larger than the result of Nussbaumer and Storey (1979). The latter two efforts were based on the distorted wave approximation, a method not noted for considerable accuracy (see Mendoza 1983). The new collision strength from Butler and Storey is based on a four-state close coupling approximation using new target wave functions and may be considered superior to the preceding calculations. Uncertainty in the atomic data for N^{++} has historically been a weakness in the N/O analysis (see Paper I). As a result of these new calculations, we believe that all the physical constants on which our study is based are reliably determined.

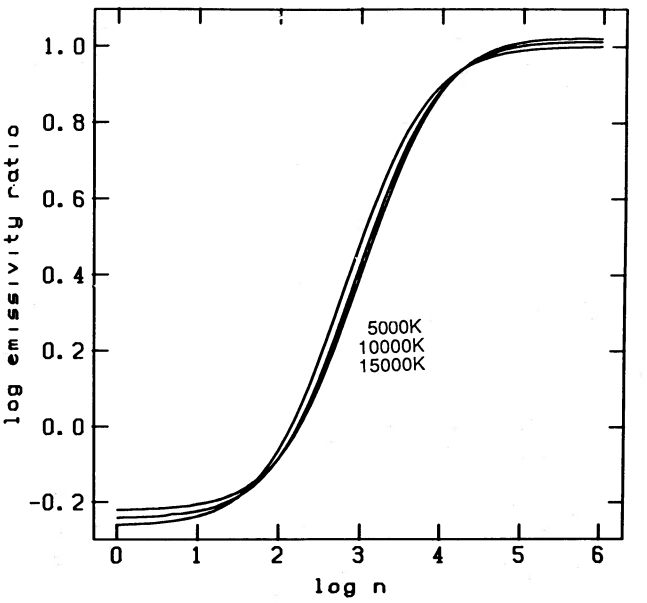

FIG. 5.—Volume emissivity ratio of [O III] 51.8 μm/[O III] 88.4 μm as a function of electron temperature and electron density.

As discussed in Paper I, *even in the strict absence of any information about electron density or electron temperature, the N^{++}/O^{++} abundance ratio is equal to the 57.3 μm/51.8 μm line intensity ratio within ±50%* (see Fig. 5). The similarity in wavelength of these latter two lines ensures that the ratio of their equivalent widths gives essentially the same information as their fluxes and justifies the comparison of fluxes measured with the same focal plane aperture without extensive correction for diffraction. As we will show below, the range of electron densities and temperatures that we encounter in this sample of H II regions is not very large and, *in practice*, the abundance ratio equals the line ratio to within about ±25%. These properties, as well as the intrinsic lack of sensitivity to intervening extinction that is a property of all far-infrared lines, make this line ratio a particularly powerful one for determining this ionic abundance ratio in H II regions. In Table 1 we summarize the more important physical constants for both ions; the collision strengths are given here only for the intermediate case of $T = 10{,}000$ K.

Figures 3, 4, and 5 and the line fluxes in Table 3 were used to generate electron densities and N^{++}/O^{++} ratios, which are listed in Table 4. The derived ratios range from less than 0.03 in 30 Doradus to almost 1.4 in G337.1−0.4. Observational errors were propagated through the nonlinear dependences to obtain the indicated errors. The emissivity ratios that were used for each source take into account the (very small) effect of electron temperature. The LTE radio recombination line electron temperatures for these sources, listed in column (5) of Table 4, were used for this correction. In the case of G337.1−0.4, no electron temperature determinations have been made, and we have assumed a value of 7000 K, which is representative of sources in that part of the Galaxy. Only one [O III] line was measured in G75.84−0.4, and therefore no electron density was derived, so we have taken an electron density $\log n_e = 4.3$, which is indicated by the [S III] observations of Herter *et al.* (1982). Similarity of the ionization potentials of O^{++} and S^{++} justifies our assumption that the [S III] electron densities are appropriate to the [O III] emitting region, as does the similarity of the derived densities for those few objects that have been observed in all four lines (see below). The resulting error in N^{++}/O^{++} for G75.84−0.4 has, however, been increased to reflect the uncertainty in this substitution.

For G333.6−0.2 and 30 Doradus, where multiple positions were observed, the derived electron densities track the ionized column density as indicated by the radio continuum surface brightness fairly well. For the 30 Doradus region, the electron density at the two radio peaks (Mills, Turtle, and Watkinson 1978) is significantly higher than that at the neighboring position centered on R136a, where the large-beam radio surface brightness is considerably smaller. This correlation of electron density and column density suggests that regions of increased column density are due to higher local electron density rather than simply greater line-of-sight thickness.

The [O III] electron densities listed in Table 4 are fairly uniform and are in general smaller than those densities inferred from radio continuum measurements of H^+ emission measure. The difference between local and global measurements of electron density can be understood at least in part as the result of incomplete filling of the volume by otherwise uniformly dense clumps. At electron densities much greater than the critical

TABLE 4

DERIVED PROPERTIES

Source (1)	N^{++}/O^{++} (2)	log n_e (cm^{-3}) (3)	He^+/H^+ (4)	T_e^* (K) (5)	$^{12}C/^{13}C$ (6)
G0.0+0.0	0.75 ± 0.11	3.9 ± 0.3	0.095 ± 0.04 (M)[a]	5000 ± 1000 (R)[b]	25 ± 5 (GW)
G0.5−0.0	1.14 ± 0.19	1.9 ± 0.2	0.062 ± 0.02 (T)[c]	5800 ± 800 (W)[d]	14 ± 5 (GW)
G10.2−0.4	0.32 ± 0.05	2.3 ± 0.1	0.054 ± 0.01 (T)[e]	5500 ± 200 (W)[d]	50 ± 15 (MP)
G15.0−0.7	0.22 ± 0.03	2.8 ± 0.1	0.102 ± 0.005 (L)[f]	6900 ± 300 (W)[d]	53 ± 9 (H)
G25.4−0.2SE	0.72 ± 0.12	2.7 ± 0.1	0.066 ± 0.010 (C)[g]	6000 ± 200 (W)[d]	...
G30.8−0.0	0.44 ± 0.07	2.6 ± 0.1	0.097 ± 0.015 (T)[c]	6500 ± 200 (W)[d]	42 ± 6 (H)
G49.5−0.4	0.26 ± 0.04	3.8 ± 0.3	0.103 ± 0.01 (T)[c]	6500 ± 400 (W)[d]	70 ± 11 (H)
G75.8−0.4	0.42 ± 0.24	4.2 (He)[h]	0.052 ± 0.013 (C)[f]	8540 ± 360 (V)[i]	...
G111.5+0.8	0.36 ± 0.07	2.5 ± 0.1	0.063 ± 0.02 (T)[c]	9000 ± 1000 (W)[d]	57 ± 2 (H)
G133.7+1.2	0.23 ± 0.04	3.3 ± 0.1	0.074 ± 0.01 (T)[c]	7600 ± 300 (W)[d]	91 ± 16 (H)
G209.0−19.3	0.31 ± 0.03	3.2 ± 0.1	0.091 ± 0.005 (T)[c]	8470 ± 380 (L)[e]	96 ± 5 (Sc)
G333.6−0.2	0.68 ± 0.11	3.5 ± 0.2	0.045 ± 0.005 (L)[f]	6900 ± 200 (Mc)[j]	64 ± 20 (H)
G337.1−0.4	1.36 ± 0.30	3.0 ± 0.2	...	...	...
30 Dor Pk1	0.03 ± 0.014	2.3 ± 0.2	0.083 ± 0.08 (S)[k]	9400 ± 500 (S)[l]	...
30 Dor Pk2	0.108 ± 0.077	2.2 ± 0.2	...	9400 ± 500 (S)[l]	...
R136a	...	1.7 ± 0.4	...	9400 ± 500 (S)[l]	...

[a] 109α; 10′ beam.
[b] 65α; 1′.3 beam.
[c] 66α; 0′.7 beam.
[d] 76α; 1′.0 beam.
[e] 76α; 0′.9 beam.
[f] 86α; 3′.5 beam.
[g] 109α; 2′.6 beam.
[h] [S III] 0′.33 beam.
[i] 85α; 2′.8 beam.
[j] 76α; 2′.3 beam.
[k] Optical lines.
[l] 109α; 4′.5 beam.

REFERENCES.—(He) Herter *et al.* 1982; (M) Mezger and Smith 1976; (T) Thum, Mezger, and Pankonin 1980; (L) Lichten, Rodriguez, and Chaisson 1979; (C) Churchwell *et al.* 1978; (S) Shaver *et al.* 1983; (R) Rodriguez and Chaisson 1978; (W) Wink, Wilson, and Bieging 1983; (V) Viner, Clarke, and Hughes; (Mc) McGee and Newton 1981; (GW) Gardner and Whiteoak 1982; (MP) Martin-Pintado *et al.* 1984; (H) Henkel, Wilson, and Bieging 1982; (Sc) Scoville *et al.* 1983.

density of a collisionally excited transition, the volume emissivity of the ion is proportional to n_e, while it is proportional to n_e^2 in the low-density limit. As a result, in a volume of gas with a range of electron densities the observed flux in a collisionally excited line will be biased toward the critical density, and the contribution of dense clumps will be deemphasized. Thus, with critical densities in the range 10^2–10^3 cm^{-3}, it is not surprising that the two far-infrared oxygen lines indicate electron densities of this order for a wide range of sources. Shorter wavelength transitions, with generally larger critical densities, might be expected to indicate larger electron densities for the same sources in the same beam size. The excellent correspondence between our O^{++} densities and the S^{++} densities of Herter *et al.* (1984) for Sgr A and Orion suggests, however, that a two-phase model, with constant density clumps embedded in a lower density medium occupying much of the volume, is appropriate to these sources. In the case of W3, however, the O^{++} electron density is a factor of 10 lower than that from S^{++}. This may indicate that a simple two-component model is inappropriate for this source, and a more complicated density structure is implied. Future observations that are better matched in beam size will, when combined with the global density measurement from the radio continuum flux, provide quantitative data on the density spectra in H II regions. We point out that, although measurements of different line ratios may give different electron densities, the far-infrared [O III] electron density is the most appropriate to this study of N^{++}/O^{++}, because the emission from N^{++} is presumably weighted similarly to that from the O^{++} ion.

IV. N^{++}/O^{++} AND N/O

Having derived N^{++}/O^{++} for galactic H II regions at a large range of galactocentric distances, we now address the relationship between the ionic ratio N^{++}/O^{++} and the elemental ratio N/O. In Paper I we argued on the basis of the similarity between the ionization potentials of N^+ and O^+ that regions in which N^{++} and O^{++} predominate are largely coextensive. This assumption, which we justified on the basis of nebular ionization structure models of Grandi and Hawley (1978), is commonly used in optical studies of N^+/O^+. With this simple assumption, that $N^{++}/O^{++} \approx N/O$, the N/O ratio was found to be at least a factor of two higher than the solar neighborhood ratio as derived from optical N^+/O^+ observations of nearby H II regions.

Recent work by Stasinska (1982) and Rubin (1985) has given new theoretical insight into the possible source of this difference. His models show that the N^{++} and O^{++} Strömgren spheres begin to decouple for very low ionization temperatures, with the result that $N^{++}/O^{++} > N/O$. For G333.6−0.2, in particular, there is some indication from these models that opacity in the nebular ionization continua of the more abundant light metals will substantially cool the ionizing radiation that is seen by much of the nebula, and this produces a similar result (Rubin 1983). G333.6−0.2 is a somewhat extraordinary case, however, since it is extremely luminous as well as ionized by a cool central source, and the ionized region is large enough to build up substantial optical thickness in the O^+ ionization continuum from center to edge. We note that

for the less luminous H II regions modeled by Simpson and Rubin (1984), of which Orion, G75.8−0.4, and W3 are included in our sample, the N^{++} and O^{++} regions are expected to be reasonably coincident. Heavy-element continuum opacity is unlikely to be the explanation for the elevated N^{++}/O^{++} in the Orion nebula for another reason. If it were, optical measurements of N^{+}/O^{+} would show a reflected effect, which is not evident from the observed data (Peimbert and Torres-Peimbert 1977). Simpson *et al.* (1986) present spatially resolved, fine-structure line measurements of the Orion nebula that confirm our data for that object and underscore the fact that N^{++}/O^{++} is about twice the accepted, optically inferred value of N/O for that object. After considering and rejecting the various explanations for this effect in a model-consistent context, these authors conclude that the optical N/O value is most likely underestimated by a factor of 2 for this object. Part of this discrepancy may be due to a more subtle effect, involving cascades following recombination from O^{+2}, which appears to raise the derived N^{+}/O^{+} over that inferred from a simple picture of collisional excitation, an effect which could result in an enhancement of this optically determined ratio by as much as 50% (Rubin 1986).

Can differences in nebular ionization explain the large N^{++}/O^{++} variations that we see without resorting to abundance differences? There is relatively little observational data that can be brought to bear on this question. Radio recombination line measurements of He^{+}/H^{+} are available for most of the H II regions in our sample, however, and provide uniform information on the degree of ionization. Although, as pointed out by Rubin (1983), He^{+}/H^{+} is not an ideal indicator of ionizing radiation in the O^{+} and N^{+} continua, it is one of very few ionization indicators measured for most of the H II regions in our sample. While the He^{+}/H^{+} ratio cannot be completely isolated from the issue of difference in elemental abundance, He/H is expected to vary much more slowly with stellar nucleosynthesis than ratios of heavier species because of the substantial primordial contribution to He that dilutes the stellar contribution. The grid of models by Stasinska (1982) generally indicate that He^{+}/H^{+} = He/H for those nebular excitation conditions for which N^{++}/O^{++} = N/O. The radio recombination line determinations are listed in Table 3 and plotted against N^{++}/O^{++} ratio in Figure 6. This figure shows that there is only a weak dependence, if any, of our derived N^{++}/O^{++} on nebular ionization. We note that the far-infrared line measurements 40″ N from the center of G333.6−0.2 show an N^{++}/O^{++} ratio that is nearly identical to that at the central position. Such a correspondence is not easily reconciled with the radial ionization gradient models that have been produced for this object.

In summary, there are several competing processes which can modify the simple picture of $N^{++}/O^{++} \approx$ N/O. The effect of low-excitation temperature and heavy-element continuum opacity on the ionizing spectrum seems to be important for only a small subset of our sample, perhaps only for G333.6−0.2. Errors in the atomic constants introduce errors in the absolute derived abundances though we argue that, as a result of recent calculations, these uncertainties are probably very small. We note that, to first order, errors in the atomic parameters for N^{++} and O^{++} will change the values derived above by a scaling factor, and a study of N^{++}/O^{++} *variations* may be undertaken independently of perfect knowledge of the absolute abundance ratio. Bearing in mind the need for a more sophisticated analysis when a more complete body of observations becomes available, we discuss the significance of our present observations assuming the simple interpretation, that $N^{++}/O^{++} \approx$ N/O.

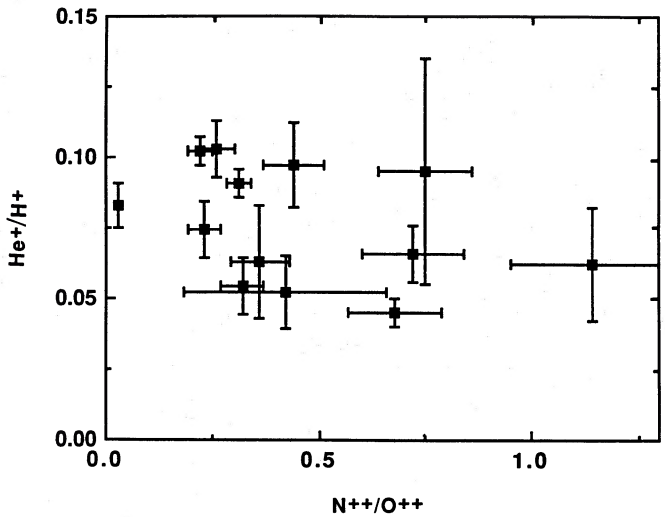

FIG. 6.—N^{++}/O^{++} vs. He^{+}/H^{+} for sources in Table 4. He^{+}/H^{+} is used here as an ionization parameter rather than an abundance indicator, as discussed in the text. Little correlation is seen, suggesting that N^{++}/O^{++} is not strongly influenced by ionization effects.

V. A POSSIBLE N/O GRADIENT IN THE GALAXY: CN NUCLEOSYNTHESIS ON A GALACTIC SCALE

a) N^{++}/O^{++} *versus* R_G

In Figure 7, we have plotted N^{++}/O^{++} from Table 4 against galactocentric distance (R_G) from Table 2. This figure bears out the tentative conclusion from Paper I that N^{++}/O^{++}, and presumably N/O, is elevated in the inner galaxy relative to the solar circle. The mean N^{++}/O^{++} inside of a galactocentric radius of about 7 kpc is approximately a factor of 3 higher than outside this radius. There is some evidence, in addition, that this ionic ratio increases abruptly inside of 7 kpc. The lack of significant variation in inferred N/O

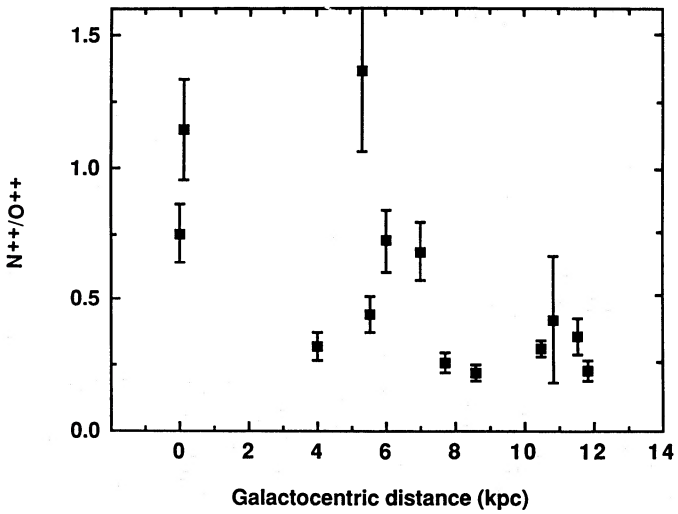

FIG. 7.—N^{++}/O^{++} vs. galactocentric distance for the sources in Table 4. An increase in N^{++}/O^{++}, and hence N/O, with decreasing galactocentric distance is evident in this plot.

between 8 and 12 kpc is reasonably consistent with the results of optical studies (cf. Peimbert 1979). While there is no information on the region between the galactic center and 4 kpc radius due to the paucity of bright H II regions there, this elevated ionic ratio appears to continue into the galactic center region.

Our observation of G0.5−0.0 is particularly important in this regard, since it suggests that an elevated N^{++}/O^{++} ratio may be a general characteristic of the entire galactic center region, and not just of Sgr A. Sgr A is a particularly extraordinary H II region in terms of its kinematical properties as well as its intimate association with the galactic nucleus, and unusual abundances seen there might otherwise be interpreted as locally enhanced nucleosynthesis rather than enrichment on a galactic scale. In addition, as described in § II above, the large velocity dispersion of the gas in Sgr A produces some added uncertainty in its line flux measurements because the line is spread over a larger wavelength interval, and the line-to-line continuum ratio is smaller than for the other sources in the sample. Interestingly, the N^{++}/O^{++} ratio in G0.5−0.0 is almost 50% larger than Sgr A itself, and it is not clear from this study which inferred N/O ratio is the most appropriate to the entire Galactic center region. This issue will be discussed in more detail below. The low electron density that we derive for G0.5−0.0 is another conspicuous attribute of this source. We note that both the extremely large N^{++}/O^{++} ratio *and* the low implied density could be accounted for simultaneously if the 52 μm line strength had been underestimated. In order to get an abundance ratio and an electron density similar to Sgr A, however, a 52 μm line more than a factor of 3 larger would have to be invoked. We consider an error of this magnitude very unlikely. It is noteworthy that G0.5−0.0 has one of the lowest He^+/H^+ ratios in our sample. A relatively low degree of ionization is thus indicated, so decoupling of N^{++}/O^{++} from N/O may be a problem for this source as in G333.6−0.2.

Our observations of 30 Doradus have not been plotted in Figure 7 because the nucleosynthetic history of the LMC is probably distinct from that of the Galaxy. The 57.3 μm [N III] line was not significantly detected in this region, and the N^{++}/O^{++} errors are dominated by noise in the data rather than by calibration errors. This region has been investigated optically, and our result that N/O is exceptionally low (<0.1) is well supported by the optical N^+/O^+ work (Pagel *et al.* 1978). Figures 1 and 2 illustrate the striking difference in mean density and N^{++}/O^{++} between different H II regions. The 30 Dor Peak 1 region in Figure 2 shows virtually no 57.3 μm [N III] line compared with its strong 51.8 μm [O III] line—an indication of very low N^{++}/O^{++}. The line observations of G337.1−0.2 can be contrasted with 30 Dor, since this object has the highest N^{++}/O^{++} ratio in the entire sample. It can also be seen that G337.1−0.2 has a higher mean density than 30 Dor, as evidenced by the relatively weak 88.4 μm line in the former object.

While N^{++}/O^{++} shows a correlation with galactocentric distance (see Fig. 7), it is clear from the scatter and error bars that a simple monotonic N/O gradient with galactocentric distance is not adequate to explain the observations. In some cases, sources with the same galactocentric distance appear to have rather different N^{++}/O^{++} abundances. In particular, G337.1−0.2 has N^{++}/O^{++} that is more than a factor of 2 higher than that of other H II regions at the same galactic circle. This could be due either to uncertainties in the observational interpretation of N^{++}/O^{++} (see § IV above) or, more significantly, to the particular way in which the Galaxy is enriched. In the latter case, it would be necessary to invoke chemical enrichment of the Galaxy on a time scale that is short compared to that required for azimuthal mixing. This possibility may be investigated by comparing our N^{++}/O^{++} measurements with other abundance indicators on a source-by-source basis. Does the scatter in N^{++}/O^{++} versus galactocentric distance result from localized parts of the galaxy in which nucleosynthesis has been very active, or perhaps from nonuniformities in the relative production rates of nitrogen and oxygen? Unfortunately, rather little information about abundances of these fairly heavily obscured H II regions is known, especially for sources inside of the solar circle, and there are no direct measurements of heavy-element abundances available for comparison with our data for the majority of H II regions in our sample. However, a number of indirect comparisons are possible, as described below.

b) N^{++}/O^{++} *Versus Inferred* O/H

It has been known for some time that H II regions in the Galaxy display a fairly strong correlation of electron temperature (as derived from radio recombination line-to-continuum measurements) with galactocentric distance, in the sense that H II regions closer to the galactic center tend to be cooler. This effect was interpreted by Churchwell *et al.* (1978) as reflecting enhanced abundances of nebular coolants (primarily oxygen) in the inner Galaxy. The observational data have been considerably refined since then and is summarized most recently by Wink, Wilson, and Bieging (1983). The dependence of electron temperature on O/H has been investigated by Mezger *et al.* (1979) and Shaver *et al.* (1983) by calibrating H II region models with nebulae for which both O/H ratios and electron temperatures are available. These latter studies indicate that a decrease in electron temperature from 8000 K to 6000 K, which is roughly the extent of the temperature gradient from the solar circle to $R_G = 4$ kpc, can be attributed to an increase in the O/H abundance by a factor of 2.5. Interestingly, there is some indication that this monotonic gradient in electron temperature does not extend all the way into the Galactic center. Although the correction for background emission is not known with certainty, Wink, Wilson and Bieging (1983) find that H II regions within 3 kpc of the Galactic center (with the arguable exception of the nuclear H II region Sgr A itself) may have $\langle T_e^* \rangle$ that is approximately 2000 K higher than that extrapolated on the basis of the gradient farther out in the disk. The electron temperature of the Sgr A H II region has been measured by Rodriguez and Chaisson (1979), though the broad lines and complicated line of sight make this measurement highly uncertain.

The LTE electron temperatures T_e^* for most of the H II regions in our sample have been taken from the literature and are listed in Table 4 along with the beam size in which they were determined. The beam size difference between the radio and infrared observations should not be of great importance since each H II region may be considered chemically homogenous, though it may be an issue if ionization effects are important in the derived abundances. We have plotted our N^{++}/O^{++} values against these electron temperatures in Figure 8. Within the errors in both measurements, there is a correlation in the sense that higher N^{++}/O^{++} corresponds to lower electron temperature and higher inferred O/H. Even excluding G0.5−0.0, which has a particularly high N^{++}/O^{++} for its low electron temperature, we find that the total range

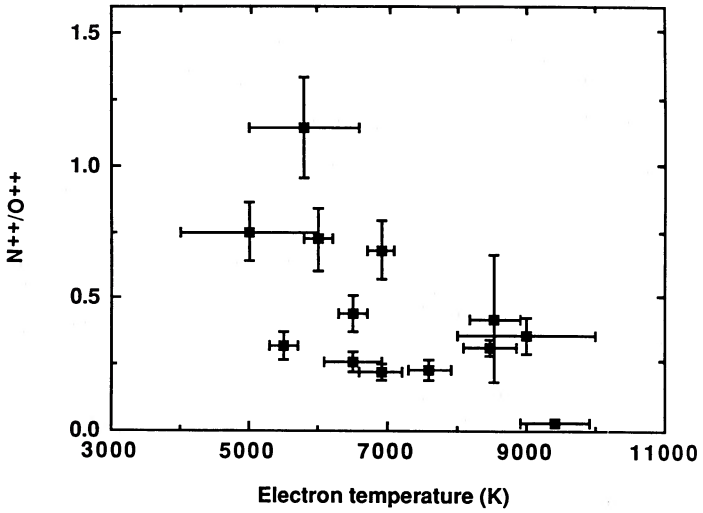

FIG. 8.—N^{++}/O^{++} vs. T_e* for the sources in Table 4. As discussed in the text, T_e* is indicative of O/H, and the observed correlation indicates $N^{++}/O^{++} \propto O/H$.

from 30 Doradus to the inner Galaxy regions, both the inferred O/H ratio and the N^{++}/O^{++} ratio increase by about a factor of 10. Regrettably, no measurement of T_e* seems to have been made for G337.1−0.4, which has the highest N^{++}/O^{++} ratio in the sample. The slope of the N^{++}/O^{++} versus T_e* relation is even larger if G0.5−0.0 is included. If $N/O \approx N^{++}/O^{++}$ with the T_e*–O/H relationship discussed above, we therefore find the N/H abundance to increase by a factor of roughly 100. Although scatter about the mean line in Figure 6 and, in particular, the extraordinarily high N/O inferred for G0.5−0.0 may indicate some variation in the relative amounts by which N and O are enriched, the main effect is consistent with relatively homogenous enrichment in which the relative stellar yields are similar from one part of the Galaxy to the other.

We point out that one should expect there to be a larger scatter in the correlation of N^{++}/O^{++} with T_e than with O/H because the sample includes regions with a range of electron densities. The electron temperature is somewhat sensitive to electron density as well as elemental abundance because of the more efficient cooling (in the infrared lines) of lower density H II regions. Such an effect can lead to differences of order 1000 K (Garay and Rodriguez 1983) compared with a more homogeneous sample.

The radial gradient of O/H in the outer Galaxy has been the subject of considerable optical emission-line work. The most recent optical evidence for an O/H gradient in the Galaxy is given by Shaver *et al.* (1983). The optical observations give direct abundance information that reinforces the much more indirect conclusions gleaned from H II region electron temperatures. Extinction in the Galactic plane has prevented optical observations from probing much closer than about 7 kpc to the Galactic center, however, and comparison of our data with electron temperature inferred abundances is the only recourse.

c) *A Primary/Secondary Model of Galactic Enrichment*

The nature of the observed enrichment is consistent with that expected for the model of Galactic enrichment discussed by Talbot and Arnett (1973) and, more recently, by Serrano and Peimbert (1983). In this model, ^{14}N is a secondary element whose production rate via the CN-burning reaction chain $^{12}C(p, \gamma)^{13}N(e^+\nu)^{13}C(p, \gamma)^{14}N$ is proportional to the amount of ^{12}C with which the reaction chain begins. The primary species ^{12}C and ^{16}O are assumed to be synthesized directly from primordial constituents by α-process nucleosynthesis in supernovae and their massive star progenitors. Assuming, in addition, that the enrichment and efficient mixing of oxygen and carbon into the interstellar medium takes place on a time scale short compared to the time scale for star formation, we predict $\partial(^{16}O/H)/\partial t \propto$ star-formation rate, and $\partial(^{14}N/^{16}O)/\partial t \propto \partial(^{16}O/H)/\partial t$. If the relative nucleosynthetic yields are assumed not to change with time, this model predicts time integrated abundance ratios $^{14}N/^{16}O \propto {}^{16}O/H$. Although our fine-structure line measurements do not give information that is isotope-specific, these isotopes are by far the dominant ones of their species in the interstellar medium, so we would therefore predict that $N/O \propto O/H$.

Several other observational studies are relevant to the picture described above. A similar CNO process primary/secondary pair that can be studied is $^{12}C/^{13}C$, since ^{13}C is secondary to primary ^{12}C. Henkel, Wilson, and Bieging (1982) and Henkel, Güsten, and Gardner (1985) have found evidence for a galactic radial gradient in $^{12}C/^{13}C$ using measurements of isotopic formaldehyde absorption toward strong continuum sources. They find that the solar neighborhood value for the ratio $H_2{}^{12}CO/H_2{}^{13}CO$ is about 90, and that it decreases toward the Galactic center, with a value of approximately 50 at a galactocentric radius of 4 kpc. Gardner and Whiteoak (1982) find that this gradient extends to the Galactic center, where ratios as low as 23 are seen. Additional, but more indirect, evidence for a similar variation of the carbon isotope ratio with galactocentric distance has been shown from double-ratio arguments (cf. Wannier 1980; Frerking *et al.* 1980). Thus, the general slope of the gradient of $13C/^{12}C$ is similar to that of N/O, as expected from the primary/secondary model.

A detailed source-by-source comparison of $H_2{}^{12}CO/H_2{}^{13}CO$ with N^{++}/O^{++} can be made for many of the objects that we have observed. This is shown in Figure 9, where the carbon isotope data are from the papers referenced above. The points in this figure indicate H II regions for which both N^{++}/O^{++} and $H_2{}^{12}CO/H_2{}^{13}CO$ measurements are available (the latter corresponding to associated molecular clouds with nearly the same radial velocity as for the H II region). The isotopic ratio estimates suffer from some inaccuracies due to optical depth effects (cf. Martin-Pintado *et al.* [1985] for G10.2) and the possibility of chemical fractionation, and we must therefore use the results with some care. For Sgr A, the isotopic ratio used is that which seems to be representative of the nuclear region of the Galaxy from the work of Gardner and Whiteoak (1982). Although there is considerable line-of-sight confusion, the velocity information from the latter measurements give some assurance that these ratios really apply to the central region of the Galaxy. The isotopic ratio for Orion is from the near-infrared absorption-line measurements of the BN source (Scoville *et al.* 1983). We assume that this isotopic ratio typifies that in the Orion molecular cloud and has not been altered by outflow from the BN star. We have attempted to increase the data set slightly by including the −39 km s^{-1} formaldehyde cloud in front of Cas A, having assumed that it has carbon isotopic abundances that are similar to that of NGC 7538, which is nearby on a galactic scale, but is not intimately associated with that H II region.

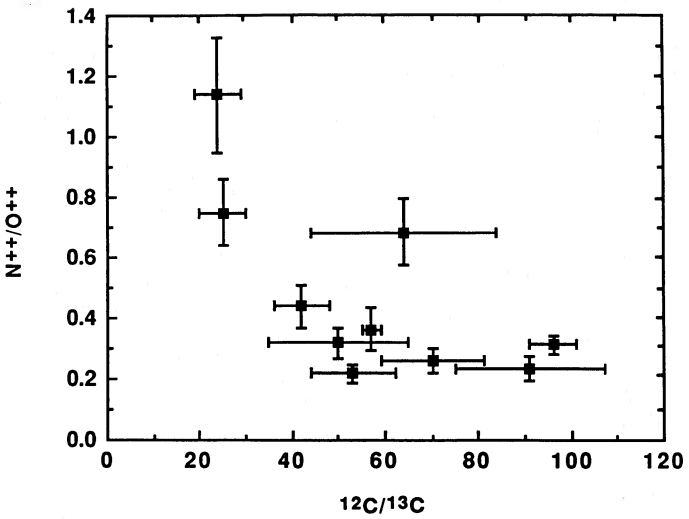

FIG. 9.—N^{++}/O^{++} vs. inferred $^{12}C/^{13}C$ for the sources in Table 4. There is strong evidence for the inverse correlation that is expected from the accumulated products of CN processing.

The expected inverse correlation between inferred N/O and $^{12}C/^{13}C$ is borne out strikingly well. The most discrepant point is that of G333.6 (at $N^{++}/O^{++} = 0.68$, $^{12}C/^{13}C = 64$) which was only marginally detected in $H_2{}^{13}CO$, and whose N^{++}/O^{++} ratio is thought (Rubin [1983] and above in § IV) to be somewhat in excess of its true N/O. We regard this good correlation as some of the strongest evidence in support of our assertion that normal CN processing has been primarily responsible for the chemical evolution of these ratios in the inner Galaxy.

Our conclusion that a secondary enrichment process best explains the behavior of N/O in the inner Galaxy can be contrasted with recent studies of very low metal abundance extragalactic H II regions (Dufour 1984) and planetary nebulae in the Galactic halo (Peimbert and Sarmiento 1985). These optical measurements indicate that $N/H \propto O/H$ in these metal-poor objects, suggesting a primary source for nitrogen. We can reconcile these optical observations of metal-poor nebulae with our measurements of more thoroughly processed gas, if secondary enrichment of nitrogen begins to dominate later in the nucleosynthetic history of a given parcel of gas. Serrano and Peimbert (1983) have found that models incorporating a major secondary component in the production of nitrogen provide the best fit to the general pattern of abundance trends going from metal-poor to metal-rich galaxies.

The lack of *direct* measurements of α-process abundances in the inner Galaxy is beginning to be remedied by infrared emission-line studies at shorter wavelengths. The dominant ions of argon, sulfur, and neon have fine-structure transitions that have been used to investigate galactic abundances. Pipher *et al.* (1984) and Simpson *et al.* (1987) have measured ionic abundances of a number of H II regions around the Galaxy. The ^1p and ^5p transitions of these ions have poorly determined atomic parameters (see Mendoza 1983), and improved atomic structure calculations would be of great value here. Although there is considerable spread in the data that may correspond to real azimuthal abundance inhomogeneities, H II regions within 4 to 7 kpc galactocentric distance show, in the mean, abundances that are a factor of 2–3 higher than for H II regions at larger radii. Of the Pipher *et al.* (1984) sample, only the inner Galaxy H II region G25.4−0.2 is common to our data set, and its enhancements in neon, sulfur, and argon are similar (roughly a factor of 2–3) to that of the inferred N/O. In addition, while their total data set of 15 regions includes only three objects at $R_G < 7$ kpc, there is some indication that the abundances (particularly of neon) may jump by a factor of 2–3 inside of this radius. Their neon abundances are probably the most accurate of their data set since the neon lines are outside the silicate features and, even for heavily obscured sources, are therefore relatively unaffected by extinction. The possibility of a sudden increase in Ne/H at the edge of the 5 kpc "ring," similar to that which we see in N/O, is intriguing. These observations reinforce the case for enhanced α-process nucleosynthesis in the inner Galaxy from the radio electron temperature measurements.

d) The Galactic Center

A recent study by Güsten and Ungerechts (1985) finds that $^{14}N/^{15}N$ is about a factor of 4 higher in the Galactic center than in the solar neighborhood. Since ^{15}N is neither produced nor destroyed in normal CNO processing, one interpretation of the inferred N/O enhancement is that of CN process enrichment of ^{14}N alone. Our N^{++}/O^{++} measurement of 1.14 for G0.5−0.0 is the second largest in our sample, and it is significant that its $^{12}C/^{13}C$ value of ∼25 is among the lowest that has been observed for gas in star-forming regions. If we are to conclude from our analysis of G0.5−0.0 in particular that N/O is very high in the entire Galactic center region and that chemical processing has been especially active there, then a departure from the simple model is necessary to reconcile this with the similarity of the electron temperature of this region with that of H II regions at 4–7 kpc where the mean N/O abundance is lower. The implication is that excess nitrogen enrichment has taken place in G0.5−0.0 relative to oxygen. Such an enrichment pattern might be expected from a stellar population weighted heavily by lower masses, in which CN processing continues without the added benefit of supernova-produced oxygen. Such a situation need not demand an unusual initial mass function. An old stellar population like that in the Galactic bulge will not only fail to produce much new oxygen, but will actually tend to *lower* the O/H in the associated interstellar medium, as quiescent ejection of relatively unprocessed stellar envelope material from the remaining lower mass stars dilutes the gas. This picture is supported by the fact that low values of $^{12}C/^{13}C$ are seen in the entire Galactic center region (Gardner and Whiteoak 1982; Penzias 1980). In the case of the molecular ring, measurements of the infrared excesses of star-forming regions do not support the idea of an unusual initial mass function, although there may be evidence for the presence of an older population (Lester *et al.* 1985).

The observation by Lester *et al.* (1981) of enhanced argon in Sgr A fits well into the general picture of enhanced N/O in the Galactic center region. To the extent that the low electron temperature derived for Sgr A can be believed, and a concomitant enhancement in O/H of a factor of 2–3 over solar can be inferred, the observed enhancement of Ar/H is understandable. Massive stars that produce argon may be expected to produce oxygen as well, though the inverse may not be true. Barker (1983) finds that in the metal-poor population of the globular cluster M15, argon, sulfur, and iron peak enrichment has lagged behind that of oxygen. Improved measurements of Galactic center abundances, including better electron tem-

perature measurements, will be essential for a thorough understanding of this region. One may speculate on the role that the possible embedded $\sim 10^6\ M_\odot$ black hole (Lacy, Townes, and Hollenbach 1982; Crawford *et al.* 1985) has had on the nuclear evolution of the gas in this extraordinary H II region. It is a little surprising that this object, rather than G0.5−0.0, has abundances that are more in accord with the large-scale abundance gradient derived from sources outside the Galactic center region.

e) The 5 kpc "*Ring*"*: a Long-Lived Feature of the Galaxy?*

As the result of generations of stars enriching the interstellar medium, elemental abundance ratios can give information about the history of star formation. It was noted briefly above that the plot of N^{++}/O^{++} versus galactocentric distance shows some evidence for a sharp rise just inside of $R_G = 7$ kpc. This indicates that, on the evolutionary time-scale of the stars that were responsible for this enrichment, star formation has been particularly active inside this galactocentric radius. Interestingly, we see evidence for prodigious contemporary star-forming activity in this same region of the Galaxy. Figure 10 compares the radial distribution of ionized gas emission (which is indicative of the current formation rate of massive stars) with derived N^{++}/O^{++} values and illustrates this similarity. We have rescaled the radial volume emissivity to normalize it to the N^{++}/O^{++} data in this figure. The radial distribution of the ionized gas was taken from the work of Güsten and Mezger (1982), who used a simple azimuthally symmetric model to deconvolve the observed line-of-sight emission measures into volume emissivity as a function of radius. This remarkable concentration of H II regions and warm molecular gas that is seen between galactocentric radii of 4 and 7 kpc has been referred to as the Galactic "ring," though it has been interpreted by some as a spiral arm.

Interpretation of the radial distributions of ionized gas and N/O abundance requires that we have some understanding of the relative yields of ^{14}N as a function of stellar mass and lifetime. While there is considerable uncertainty about the sites of ^{14}N production, when theoretical yields are integrated over reasonable initial stellar mass functions masses of order 3–10 $M_\odot$, with main-sequence lifetimes of order 10^7–10^8 yr emerge as being the most important (see, e.g. Serrano and Peimbert 1983). Studies of 15–25 $M_\odot$ progenitor supernova nucleosynthesis (Weaver, Zimmermann, and Woosley 1978) suggest that ^{14}N is not efficiently produced by such stars compared with less massive stars which eject ^{14}N in planetary nebula or nova episodes (Peimbert and Sarmiento 1985). Our observations thus suggest that star formation at 5 kpc galactocentric radius must have been exceptionally efficient more than 10^7 yr ago, in order to have substantially enriched the interstellar medium there in secondary products. This implies that the "ring" has a lifetime approaching that of a Galactic rotation period.

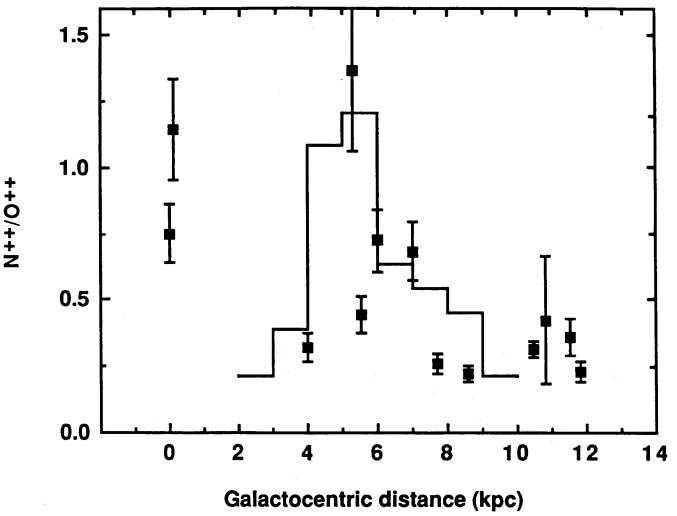

FIG. 10.—Same as Fig. 7, except with the addition of a curve showing the run of ionized gas emission with galactocentric distance. The latter curve is indicative of OB star density and thus shows the radial distribution of current star-formation rate in the Galaxy. The peak in OB star density indicates the 5 kpc "ring." A simple picture of nucleosynthesis in this "ring" indicates that it must be a long-lived feature in the Galaxy.

Large-beam, near-infrared surveys of the Galaxy show a similar enhancement at these galactocentric radii (Ito, Matsumoto, and Uyama 1977; Oda *et al.* 1979). A high volume density of red giants or supergiants is the simplest explanation for this enhancement and supports the picture of a historically high star-formation rate. Such stars, in fact, are part of the population that accounts for the enrichment that we see.

Galactic rotation curves and studies of molecular emission indicate that the fractional mass of gas in the galactic "ring" is similar to that of the solar neighborhood (cf. Güsten and Mezeger 1982). The relatively high gas density is easily reconciled with the currently high rate of star formation per unit volume. Compared with the solar neighborhood, the elevated abundances of the inner galaxy imply a historically high rate of star formation there. These facts argue that the inner galaxy is not a closed system for, if it were, successive generations of star formation would deplete the reservoir of available gas and increase the stellar density. In a closed system, it can be shown that the gas mass fraction decreases with increasing nucleosynthetic enrichment as more and more gas is tied up in long-lived stars at the low-mass end of the initial mass function. We thus have some evidence for replenishment of gas in the 5 kpc ring on a time scale similar to that required for nucleosynthetic enrichment. It is possible that infall from the galactic halo is the source of this additional gas.

VI. SUMMARY

Measurements of the far-infrared lines [O III] 51.7 μm, 88.4 μm and [N III] 57.3 μm are presented for 13 H II regions covering a wide range in galactocentric distance. These lines are used to derive electron densities and N^{++}/O^{++} abundance ratios. We argue that this ionic ratio is indicative of the elemental ratio N/O. The far-infrared data allow us to probe the N/O abundance ratio in regions of the Galaxy that are inaccessible to optical or UV measurements because of extinction. Thus we have been able to carry out the first truly *global* survey of N/O abundances in the Galactic disk.

It is shown that, using new atomic constants for these transitions, the line flux ratio 57.3 μm [N III]/51.7 μm [O III] is very nearly equal to the N^{++}/O^{++} abundance ratio and is only weakly dependent on nebular conditions. The wavelength proximity of these two lines offers special observational advantages, making this line ratio a powerful tool for investigating chemical abundances in H II regions.

Our derived N^{++}/O^{++} values, to first order, show an inverse correlation with distance from the Galactic center. In the ring of enhanced star formation between 4 and 7 kpc from

the Galactic center, N^{++}/O^{++} is approximately a factor of 2.5 higher than for H II regions near the solar circle. There is some indication that N/O is relatively constant from 12 kpc inward to 7 kpc, which is consistent with the results of optical studies. N^{++}/O^{++} is also elevated in the Galactic center region, though it is more than twice as large in the inner-disk extranuclear H II region G0.5−0.0 as in the nuclear H II region Sgr A. The [O III] lines are also detected in the 30 Doradus complex in the Large Magellanic Cloud. The limit on N^{++}/O^{++} is at least a factor of 10 below that for the solar neighborhood, in agreement with optical measurements.

Comparison of N^{++}/O^{++} with other abundance indicators on a source-by-source basis shows significant correlations. N^{++}/O^{++} tends to increase as the H II region electron temperature decreases, a decrease that is conventionally interpreted as being due to an *increase* in the relative abundance of oxygen, the primary nebular coolant. This behavior is consistent with a model of galactic enrichment in which ^{14}N is secondary to primary ^{16}O, a scenario that is the natural result of CN processing. Additional evidence for the importance of CN processing as the dominant enrichment mechanism for ^{14}N and ^{13}C in the inner Galaxy is the good correlation of inferred N/O with $^{13}C/^{12}C$. These correlations suggest that the differences in N/O that we see around the Galaxy are indicative of different amounts of the same kind of nucleosynthesis and not due to differences in the nucleosynthetic scenarios. The importance of secondary ^{14}N has been recently questioned, however, on the basis of observations which show that for low metal abundance nebulae, N is found to follow the abundances of α-process isotopes of oxygen and carbon and that a primary source of ^{14}N is required. Our observations may be reconciled if a secondary process dominates the enrichment of ^{14}N for a relatively enriched stellar population, such as that which characterizes the inner Galaxy.

The similarity of the gas mass fraction in the inner Galaxy and solar neighborhood, along with the evidently higher historically averaged rate of nucleosynthesis in the former, may be consistent with the picture that infall of relatively unprocessed material has been important to the continued rate of star formation in the inner Galaxy.

We gratefully acknowledge the expert assistance of the staff and crew of the Kuiper Airborne Observatory. Special thanks are extended to the Australian Ministry of Science and the Richmond RAAF personnel for their support and hospitality during the 1983 KAO Australia expedition. C. Townes and M. Crawford made important contributions to all phases of the observational program. H. B. Ellis is thanked for his assistance in the data handling. Useful discussions are acknowledged with C. Mendoza, R. Rubin, J. Simpson, and G. Shields. We are grateful to K. Butler for communicating the new N^{++} collision strengths in advance of publication. This project was begun while D. F. L. and H. L. D. held National Research Council Associateships at the NASA Ames Research Center. Astronomy at the Ames Research Center is supported by the Astrophysics Division of NASA. H. L. D. acknowledges further support from the R. A. Welch Foundation, NSF grant 83-14862, and NASA Ames–University of Texas Research Interchange NCA2-34. D. F. L. received partial support from the University of Hawaii and McDonald Observatory.

REFERENCES

Aggarwal, K. M. 1983, *Ap. J. Suppl.*, **52**, 387.
Audouze, J., and Tinsley, B. M. 1976, *Ann. Rev. Astr. Ap.*, **14**, 43.
Baluja, K. L., and Doyle, J. G. 1981, *J. Phys. B.*, **14**, L11.
Barker, T. 1983, *Ap. J.*, **270**, 641.
Butler, K., and Storey, P. J. 1987, in preparation.
Churchwell, E., Smith, L. F., Mathis, J., Mezger, P. G., and Hutchmeier, W. 1978, *Astr. Ap.*, **70**, 719.
Crawford, M. K., Genzel, R., Harris, A. I., Jaffe, D. T., Lacy, J. H., Lugten, J. B., Serabyn, E., and Townes, C. H. 1985, *Nature*, **315**, 467.
Dinerstein, H. L. 1986, *Pub. A.S.P.*, **98**, 979.
Dinerstein, H. L., Lester, D. F., and Werner, M. W. 1985, *Ap. J.*, **291**, 561.
Dinerstein, H. L., Lester, D. F., Werner, M. W., Watson, D., Genzel, R., and Rubin, R. 1984 in *Airborne Astronomy Symposium*, ed. H. A. Thronson and E. F. Erickson (NASA CP 2353), p. 266.
Dufour, R. J. 1984, in *Future of Ultraviolet Astronomy Based on Six Years of IUE Research*, ed. J. M. Mead, R. D. Chapman, and Y. Kondo (NASA CP 2349), p. 107.
Frerking, M. A., Wilson, R. W., Linke, R. A., and Wannier, P. G. 1980, *Ap. J.*, **240**, 65.
Garay, G., and Rodriguez, L. F. 1983, *Ap. J.*, **266**, 263.
Gardner, F. F., and Whiteoak, J. B. 1982, *M.N.R.A.S.*, **199**, 23P.
Gatley, I., Becklin, E. E., Werner, M. W., and Wynn-Williams, C. G. 1977, *Ap. J.*, **216**, 277.
Genzel, R., Watson, D. M., Townes, C. H., Dinerstein, H. L., Hollenbach, D., Lester, D. F., Werner, M. W., and Storey, J. W. V. 1984, *Ap. J.*, **276**, 551.
Grandi, S. A., and Hawley, S. A. 1978, *Pub. A.S.P.*, **90**, 125.
Güsten, R., and Mezger, P. G. 1982, *Vistas Astr.*, **26**, 159.
Güsten, R., and Ungerechts, H. 1985, *Astr. Ap.*, **145**, 241.
Haas, M. R., Erickson, E. F., McKibbin, D. D., Goorvitch, D., and Caroff, L. J. 1982, *Icarus*, **51**, 476.
Henkel, C., Güsten, R., and Gardner, F. F. 1985, *Astr. Ap.*, **143**, 148.
Henkel, C., Wilson, T. L., and Bieging, J. 1982, *Astr. Ap.*, **109**, 344.
Herter, T., Briotta, D. A., Gull, G. E., Shure, M. A., and Houck, J. R. 1982, *Ap. J.*, **262**, 164.
Herter, T., Houck, J. R., Shure, M., Gull, G. E., and Graf, P. 1984, *Ap. J. (Letters)*, **287**, L15.
Hyland, A. R., McGregor, P. J., Robinson, G., Thomas, J. A., Becklin, E. E., Gatley, I., and Werner, M. W. 1980, *Ap. J.*, **241**, 709.
Ito, T., Matsumoto, T., and Uyama, K. 1977, *Nature*, **265**, 517.
Lacy, J. H., Townes, C. H., and Hollenbach, D. J. 1982, *Ap. J.*, **262**, 120.
Lester, D. F., Bregman, J. D., Witteborn, F. C., Rank, D. M., and Dinerstein, H. L. 1981, *Ap. J.*, **248**, 524.
Lester, D. F., Dinerstein, H. L., Werner, M. W., Harvey, P. M., Evans, N. J. II, and Brown, R. L. 1985, *Ap. J.*, **296**, 565.
Lester, D. F., Dinerstein, H. L., Werner, M. W., Watson, D. M., and Genzel, R. L. 1983, *Ap. J.*, **271**, 618 (Paper I).
Lichten, S. M., Rodriguez, L. F., and Chaisson, E. J. 1979, *Ap. J.*, **229**, 524.
Loewenstein, R., *et al.* 1977, *Icarus*, **31**, 315.
Martin-Pintado, J., Wilson, T. L., Johnston, K., and Henkel, C. 1985, *Ap. J.*, **299**, 386.
Mayor, M. 1976, *Astr. Ap.*, **48**, 301.
McGee, R. X., and Newton, L. M. 1981, *M.N.R.A.S.*, **196**, 889.
Mendoza, C. 1983, in *IAU Symposium 103, Planetary Nebulae*, ed. D. Flower (Dordrecht: Reidel), p. 143.
Mezger, P. G., Pankonin, V., Schmid-Burgk, J., Thum, C., and Wink, J. 1979, *Astr. Ap.*, **80**, L3.
Mezger, P. G. and Smith, L. F. 1976, *Astr. Ap.*, **47**, 143.
Mills, B. Y., Turtle, A. J., and Watkinson, A. 1978, *M.N.R.A.S.*, **185**, 263.
Nussbaumer, H., and Rusca, C. 1979, *Astr. Ap.*, **72**, 129.
Nussbaumer, H., and Storey, P. J. 1979, *Astr. Ap.*, **71**, L5.
———. 1981, *Astr Ap.*, **99**, 177.
Oda, N., Maihara, T., Sugiyama, T., and Okuda, H. 1979, *Astr. Ap.*, **72**, 309.
Pagel, B. E. J., and Edmunds, M. G. 1981, *Ann. Rev. Astr. Ap.*, **19**, 77.
Pagel, B. E. J., Edmunds, M. G., Fosbury, R. A. E., and Webster, B. L. 1978, *M.N.R.A.S.*, **184**, 569.
Peimbert, M. 1979, in *IAU Symposium 84, The Large-Scale Characteristics of the Galaxy*, ed. W. B. Burton (Dordrecht: Reidel), p. 307.
Peimbert, M., and Sarmiento, A. 1985, *Astr. Express*, **1**, 97.
Peimbert, M., and Torres-Peimbert, S. 1977, *M.N.R.A.S.*, **179**, 217.
Penzias, A. 1980, *Science*, **208**, 663.
Pipher, J. L., Helfer, H. L., Herter, T., Briotta, D. A., Houck, J. R., Willner, S. P., and Jones, B. 1984, *Ap. J.*, **285**, 174.
Rodriguez, L. F., and Chaisson, E. J. 1978, *M.N.R.A.S.*, **184**, 145.
Rubin, R. H. 1983, *Ap. J.*, **274**, 671.
———. 1985, *Ap. J. Suppl.*, **57**, 349.
———. 1986, *Ap. J.*, **309**, 334.
Saraph, H. E., Seaton, M. J., and Shemming, J. 1969, *Phil. Trans. Roy. Soc. London, A*, **264**, 77.
Scoville, N. Z., Kleinmann, S. G., Hall, D. N. B., and Ridgeway, S. T. 1983, *Ap. J.*, **275**, 201.

Serrano, A., and Peimbert, M. 1983, *Rev. Mex. Astr. Ap.*, **8**, 117.
Shaver, P. A., McGee, R. X., Newton, L. M., Danks, A. C., and Pottasch, S. R. 1983, *M.N.R.A.S.*, **204**, 53.
Simpson, J. P., Bregman, J. D., Dinerstein, H. L., Lester, D. F., Rank, D. M., and Witteborn, F. C. 1987, in preparation.
Simpson, J. P., and Rubin, R. H. 1984, *Ap. J.*, **281**, 184.
Simpson, J. P., Rubin, R. H., Erickson, E. F., and Haas, M. R. 1986, *Ap. J.*, **311**, 895.
Stasinska, G. 1982, *Astr. Ap. Suppl.*, **48**, 299.
Storey, J. W. V., Watson, D. M., and Townes, C. H. 1979, *Ap. J.*, **233**, 109.
Talbot, R. J., Jr., and Arnett, W. D. 1973, *Ap. J.*, **186**, 51.
Thum, C., Mezger, P. G., and Pankonin, V. 1980, *Astr. Ap.*, **87**, 269.
Tomkin, J., and Lambert, D. L. 1984, *Ap. J.*, **279**, 220.
Viner, M. R., Clarke, J. N., and Hughes, V. A. 1976, *A.J.*, **81**, 512.
Wannier, P. G. 1980, *Ann. Rev. Astr. Ap.*, **18**, 399.
Watson, D. M. 1986, *Phys. Scripta*, **T11**, 33.
Watson, D. M., Storey, J. W. V., Townes, C. H., and Haller, E. E. 1981, *Ap. J.*, **250**, 605.
Weaver, T. A., Zimmermann, G. B., and Woosley, S. E. 1978, *Ap. J.*, **225**, 1021.
Wink, J. E., Wilson, T. L., and Bieging, J. H. 1983, *Astr. Ap.*, **127**, 211.

H. L. DINERSTEIN: Department of Astronomy, University of Texas, Austin TX 78712

R. GENZEL: Max-Planck Institute for Physics and Astrophysics, Institute for Extraterrestrial Physics, D-8046 Garching, West Germany

D. F. LESTER: Department of Astronomy and McDonald Observatory, University of Texas, Austin TX 78712

J. W. V. STOREY: Department of Physics, University of New South Wales, P.O. Box 1, Kensington NSW, Australia

D. M. WATSON: Department of Physics, Downes Laboratory, California Institute of Technology, Pasadena CA 91125

M. W. WERNER: Space Sciences Division, NASA Ames Research Center, Moffett Field, CA 94035